Improved United-Atom Force Field for 1-Alkyl-3-methylimidazolium Chloride

Zhiping Liu,[†] Ting Chen, Alex Bell,* and Berend Smit*

Energy Biosciences Institute and Department of Chemical Engineering, University of California, Berkeley, Berkeley, California 94720-1462

Received: November 30, 2009; Revised Manuscript Received: February 22, 2010

We have developed a united atom (UA) nonpolarizable force field for 1-alkyl-3-methyl-imidazolium chloride ([$C_n$mim][Cl], $n = 1, 2, 4, 6, 8$), a potential solvent for the pretreatment of lignocellulosic biomass. The charges were assigned by fitting the electrostatic potential surface (ESP) of the ion pair dimers. The Lennard-Jones parameters of the hydrogen atoms on the imidazolium ring were adjusted to agree with the ab initio optimized geometries of isolated ion pairs. Molecular dynamics (MD) simulations were performed for a wide range of temperatures to validate the force field. Substantial improvements were found in both the dynamical properties and the fluid structures, as compared to those predicted using our previously developed UA force field (UA2006) (*Phys. Chem. Chem. Phys.* **2006**, *8*, 1096). Liquid densities were found to lie within 2% experimental data. The simulated heats of vaporization decreased about 30% relative to that predicted using the UA2006 force field. The site−site radial distribution functions between the hydrogen atoms on the imidazolium ring and the chloride anions were in good agreement with those determined by ab initio molecular dynamics. The newly developed force field gives a much better description of the self-diffusion coefficients and shear viscosities, which usually deviate by 1 order of magnitude when determined using other force fields.

1. Introduction

Ionic liquids (ILs) are organic salts with melting points between 298 and 373 K. Due to their negligible vapor pressure and good thermal stability, ILs have attracted increasing interest for application in fields of catalysis,[1] separations,[2] electrochemistry,[3] nanotechnology,[4] and analytical chemistry.[5] Various combinations of cations and anions make ILs "designable" solvents of great versatility for an increasing number of applications.[6]

A molecular understanding of IL properties is crucial to the design of ILs. Weingätner has recently presented an excellent review summarizing the progresses, problems, and challenges on this topic.[7] Infrared (IR),[8] Raman,[9] and nuclear magnetic resonance (NMR)[12] spectroscopy; measurements of the dielectric coefficient[10] and the Kerr effect;[11] and neutron diffraction methods[13] have been used to study the structure and dynamics of ILs on different time scales. The molecular state of ILs can be extracted from the experimental information, and this information can be used to gain insights into the unique properties of these intriguing materials.

Computer simulations can contribute to understanding the behavior of ILs at the molecular scale. The quality of such simulations, however, depends on the force field used to describe the interactions between atoms or molecules. At present, most of the force fields used to simulate ILs are pairwise-additive, do not account explicitly for polarization, and were developed by extending and refining well-established force fields, such as AMBER, OPLS, CHARMM, or GROMOS. For example, Lopes et al. have developed a series of all-atom (AA) force fields consistent with OPLS for 1-alkyl-3-methyl-imidazolium ([$C_n$mim]),[14] 1,2,3-trialkylimidazolium,[15] 1-alkoxycarbonyl-3-alkyl-imidazolium,[15] 1-alkyl-3-methyl-pyridinium ([$C_n$mpy])[16] and phosphonium[16] cations and for tetrafluoroborate ([BF_4]),[14] hexafluorophosphate ([PF_6]),[14] nitrate,[14] chloride,[16] bromide,[16] dicyanamide,[16] alkylsulfonate,[15] alkylsulfate,[15] triflate,[17,18] trifluoroacetate,[18] and bistriflylimide ([Tf_2N])[17] anions. We have proposed an AA[19] and a united-atom (UA)[20] force field using the AMBER framework for 1-alkyl-3-methyl-imidazolium with combinations of chloride, [BF_4], and [PF_6]. Various groups have extended the force field parameters to a wide range ions, including guanidinium,[21,22] triazolium,[23] and choline[24] cations and trifluoroacetate,[21] perchlorate,[21] tris(pentafluoroethyl)trifluorophosphate,[25] and 14 amino acid anions.[26]

The electrostatic interactions between the cations and anions play a crucial role in determining the properties of ILs. Most of the force fields mentioned above are based on the fixed point charge located at the center of each atom, with values assigned by fitting ab initio calculations for isolated ions in their most stable conformer. The approaches used to achieve the fit are quite different and include methods such as Mulliken population analysis (MPA),[27] restraint electrostatic potential (RESP),[19−21,26] charges obtained from electrostatic potentials using a grid-based method (CHELPG),[14−17,23,28] and distributed multipole analysis.[29] Therefore, in the force fields proposed by different groups, the charge placed on a given ion can be quite different.

Schröder and Steinhauser[30] have recently compared simulation of 1-ethyl-3-methyl-imidazolium (C_2mim) dicyanoamide using two force fields with different sets of point charge. Although the charges on the cations were quite different, they found only marginal differences in the radial distribution and orientation correlation functions. However, the dynamic properties were influenced substantially by the charge distribution. The ratio of the simulated shear viscosities for the two force fields was 1.7, and similar ratios were found for other dynamic parameters, including the relaxation time for dipole−dipole correlation, the self-diffusion coefficient, and the electrical conductivity. This

* To whom correspondence should be addressed. E-mails: (A.B.) alexbell@berkeley.edu, (B.S.) berend-smit@berkeley.edu.
[†] On leave from Beijing University of Chemical Technology, China.

10.1021/jp911337f
Published on Web 03/17/2010

indicates that the viscosity can be used as a characteristic property in the development of force fields.

The multibody nature of molecular interactions can be included in the force field by the introduction of polarization. The inducible point dipole is one of the popular implementation of polarization.[31] To the best of our knowledge, all of the published force fields for ILs that account for polarization[32−37] have used this method or its variations. Yan et al. have shown[32] that the viscosity of [C_2mim][NO_3] predicted by force field that includes the effects of polarization agrees more closely with experimental data and is about 30% lower than that obtained using a force field that does not account for the effects of polarization. Borodin et al.[35] have also found better agreement between simulated and experimentally measured viscosities of [C_2mim][Tf_2N] using a force field that includes the effects of polarization.

Although a force field including polarization usually gives better results than one excluding polarization, the computational cost for the former type of force field are much higher. Thus, the so-called "empirical" force fields with effective fixed point charges are still widely used in simulations of various systems. In addition, the results obtained using force fields that exclude the effects of polarization are sufficiently good in many cases, particularly after further parameter refinements. For example, even the simple point charge model for water yields very good predictions of both structural and dynamic properties after optimization of a few parameters.[38]

Many recent studies[35,39−48] have shown that force fields of ILs that do not contain a polarization term, and charges fitted via ab initio calculations of the isolated ions, usually result in substantially lower predictions of transport properties and overestimation of the heat of vaporization. For example, the self-diffusion coefficient of [C_2mim][BF_4] is underestimated by about an order of magnitude by two widely used force fields.[14,19] Similar observations have also been found for [$C_n$mpy][Tf_2N].[48] The viscosity of [C_2mim][Cl] using an AMBER based force field[49] has also been overestimated by an order of magnitude.[42] It has also been reported that [C_1mim][Cl] and [C_4mim][PF_6] are overstructured[40,50] when their structure is determined using the force fields reported in refs 14 and 19. Evidence of overstructuring is shown by the significantly higher peak values of the site−site radial distribution functions (RDF) for the acid hydrogen in the imidazolium ring and the anions.

Several attempts have been made to further optimize the parameters of force fields not containing a polarization term.[40,41,50−55] Ideally, one would like to use accurate quantum calculations to obtain these force field parameters directly. However, the quantum calculations can be carried out only for relatively small systems of a few molecules, which can be quite a different state as compared to a dense liquid. Therefore, it is unavoidable to further tune the parameters using available experimental data.

Köddermann et al. have presented a new force field for [$C_n$mim][Tf_2N] parametrized with respect to experimentally measured properties, including liquid density, self-diffusion coefficients of cations and anions, and rotational correlation times for imidazolium cations and for water in [C_2mim][Tf_2N].[51] Their optimization focused on the Lennard-Jones (LJ) parameters for the atoms in the anion and the acid hydrogen and their adjacent carbon atoms in the cation while the charges remained identical to those used in the force field developed by Lopes et al.[14,17] Although the adjustments were ad hoc, the agreement with experimental measurements was very good, including the shear viscosity and the heats of vaporization, which were not used in the parametrization. Logothetit et al. have proposed another force field for the same series of ILs.[54] Different conformers of isolated ion pairs were used to determine the partial charges via the CHELPG method; other parameters were extracted from CHARMM without further optimization. The total ionic charges on the cation and anion were about $\pm 0.88e$, instead of $\pm 1e$, due to the polarization between the cation and anion. The simulated liquid densities and self-diffusion coefficients were in good agreement with the experiments. A similar strategy for assigning the charges has been used by other groups. Morrow and Maginn[28] have developed a force field for [C_4mim][PF_6] in which the total ionic charges are $\pm 0.904e$. In the force fields for ILs proposed by Lee et al.,[18] which include fluorinated organic anions such as CF_3COO^- and $CF_3SO_3^-$, the total charges on the cation and anion range from $\pm 0.85e$ to $\pm 0.90e$.

Bhargava and Balasubramanian[50] have optimized the charges (and also a few LJ parameters) to reproduce the RDFs obtained by Car−Parrinello molecular dynamics (CPMD).[56] They chose ± 0.8e as the charges on the cation and anion of [C_4mim][PF_6]. It should be noted that the partial charges in their force field were generally lower than those by ESP fitting of either isolated cation[14] or ion pair.[28] The simulated densities of the liquids, self-diffusion coefficients, and surface tension by the optimized force field agreed very well with experimental measurements, whereas the simulated viscosity was below the experimental value by 25−40%.[53]

Youngs et al.[4041]have also used the results of ab initio MD (AIMD)[57] or CPMD simulations[58,59] to develop the force field for [C_1mim][Cl]. In this study, the authors optimized all of the force field parameters, including the intramolecular ones using a force-matching method. They found that the structure obtained by AIMD could not be reproduced unless the total charges on the cation and anion were scaled down to ± 0.8e or lower. Their final optimized force field[41] gave value cation and anion charges of ± 0.79e, the use of which resulted in self-diffusion coefficients that were about 30 times higher than those obtained using ionic charges of ± 1e. However, the entire parameter set in the optimized force field was quite different from those found for the well-established force fields such as CHARMM and AMBER, and consequently, it is unclear whether the force field can be transferred to other ILs.

In summary, most of the nonpolarized force field optimizations indicate the occurrence of charge transfer ranging from 0.1 to 0.3e, depending on the strength of the interactions between the cations and anions. The dynamics properties can be significantly improved by scaling down the total charges on cation and anion.

In this work, we propose a new united-atom (UA) force field for alkylimidazolium chloride ([$C_n$mim][Cl]), ILs that have been identified as good solvents for cellulose.[60] This force field involves partial charges derived from RESP fitting to dimers of an ion pair but does not contain an explicit term to account for polarization. The LJ parameters of the acid hydrogen on the imidazolium ring were adjusted to reproduce the optimized geometries of different ion pair conformers. A UA force field was chosen because it decreases the computational cost by a factor of 1/4 as compared with an AA force field.[20] The densities of the liquids, heats of vaporization, microscopic structures, self-diffusion coefficients, and shear viscosities were simulated using the optimized force fields and compared with experimental values where available.[61,62]

2. Computational Details

2.1. Ab Initio Calculations and Charge Fitting. All the ab initio calculations were performed using the Gaussian03 program.[63] The B3LYP hybrid DFT method was used in geometry optimizations with the 6-31G+(d,p) basis set (the keywords "scf=tight" and "int=ultrafine" were used in the calculations to get better convergence). Additional vibration analysis was carried out to ensure the absence of negative frequencies and verify the existence of a true minimum. The electrostatic potential surface was generated by the Merz−Kollman (MK) method at the B3LYP/cc-pVTZ level, followed by a two-stage RESP[64] fitting. All the atom charges were optimized at the first stage, and the charges on equivalent atoms (for example, the same type atom in the ion pair dimer) were restricted to be the same at the second stage. The restraint weight factors were chosen as 0.005 and 0.001 at the two stages, respectively. As in our previously developed UA force field,[20] the hydrogen atoms on the alkyl groups were not included in the fitting.

Ab initio calculations of the dihedral energy profile were performed at the MP2/cc-pVTZ//B3LYP/6-31+G(d,p) level. During the geometry optimization, all the degrees of freedom were adjusted, except for the dihedral angle of interest, which was varied in steps of 10°. The molecular mechanics (MM) package, TINKER, version 4.2,[65] was used to produce the same dihedral energy profile by the force field. At first, the coefficients related to the dihedral were set to zero. Thus, a preliminary set of dihedral coefficients could be fitted by the difference between the ab initio and MM calculations, with which an updated MM dihedral profile was obtained. The procedure typically iterated two to three times to get a converged difference between the ab initio and MM energies.

2.2. Molecular Dynamics Simulations. All the MD simulations were implemented using the parallel LAMMPS package.[66] The time step was set to 2 fs and the velocity−Verlet algorithm was used to integrate the equations of motion. The SHAKE algorithm was applied to all the bonds and angles related to hydrogen, with a tolerance of 10^{-4} and maximum iteration of 10. The neighbor lists were built with a skin distance of 0.2 nm every 5 steps. A cutoff of 1.2 nm was set for both the LJ and Coulombic interactions. The LJ tail correction was added to the energy and pressure, and the long-range electrostatic interactions were dealt with using the particle−particle particle-mesh solver. The temperature and pressure were controlled by a Nosé-Hoover thermostat and barostat, with update frequencies of 0.2 and 2 ps, respectively.

A total of 250 ion pairs were included in each simulation, and a larger system involving 500 pairs was used in a few simulations to verify the size effect. The initial state was prepared by PACKMOL[67] in a cubic box, typically much larger than its "real" size, followed by a conjugate gradient energy minimization within 1000 steps. It is well-known that the dynamics of ILs are very slow and the simulation results probably depend on the initial state. Thus, the system was heated to 800 K, and NPT runs were carried out to 500 ps to improve the dynamics and overcome the possible energetic trapping. Several independent runs were also performed to confirm the results were independent of the initial state. The system was then cooled from 800 K (typically 50 K/10 000 steps) to the target temperature, followed by 1 ns equilibrium NPT runs. Another 2 ns NPT run was performed to obtain ensemble-averaged intermolecular energies and liquid densities. Additional 2 ns NVT runs were carried out at the average liquid density to estimate the self-diffusion coefficients. The snapshots of atoms were stored every 0.5 ps for postanalysis.

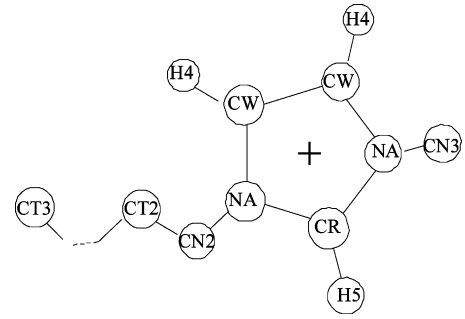

Figure 1. Schematic structure and atom type notations for [$C_n$mim] cations.

For the viscosity calculations, NVT runs were carried out for more than 10 ns to equilibrate the system, leading to a stable pressure of around 0.1 MPa. Subsequently, at least 20 ns NVT production runs were carried out to ensure that the statistical sampling was adequate. The nine components of the pressure tensors were recorded at every time step, and trajectories of 20 ns were used to compute the viscosity (see section 4.4 for details). In computing time-correlation functions, we used the multiple time origin average method to improve the statistics.

3. Force Field Development

3.1. Functional Form, Atom Types and Intramolecular Coefficients. The classical functional form of the force field, including bonded (the first three terms) and nonbonded (the last two terms) parts, was adopted. This form is identical to that used in our previous work,[20]

$$U = \sum_{\text{bonds}} K_r(r - r_0)^2 + \sum_{\text{angles}} K_\theta(\theta - \theta_0)^2 + \sum_{\text{dihedrals}} K_\chi[1 + \cos(n\chi - \delta)] + \sum_{i<j} 4\varepsilon_{ij}[(\sigma_{ij}/r_{ij})^{12} - (\sigma_{ij}/r_{ij})^6] + \sum_{i<j} q_i q_j / r_{ij} \quad (1)$$

in which K_r, K_θ, and K_χ are energy coefficients of the bonds, angles, and dihedrals, respectively; ε_{ij} and σ_{ij} are the energy and size parameters between atoms i and j in the LJ potential; and q_i is the charge on atom i. The nonbonded interactions were scaled by a factor of 0.5 for atoms separated by three consecutive bonds (1−4 interactions) and ignored for atoms separated by less than three consecutive bonds.

To decrease the computational cost, we define the alkyl groups CH_2 and CH_3 as the united atoms. As discussed in our previous work,[20] the hydrogens in the imidazolium ring, that is, H4 and H5, are not treated as united atoms because these are more active as compared to those in alkyl groups. The hydrogen atoms have an important role in forming the hydrogen bonds in ILs. The LJ parameters of the united atoms were extracted from our previous work[20] without modification. The Lorentz−Berthelot combining rules were used to obtain the cross parameters for interactions between unlike atoms.

The AMBER-style atom types were assigned for the cations [$C_n$mim] in a manner identical to that used previously[20] with the notation shown in Figure 1. The bond stretching and angle bending are weakly coupled with other interactions in the molecules, such as torsion, VDW, and Coulomb interactions. In this work, the equilibrium bond lengths and angles are

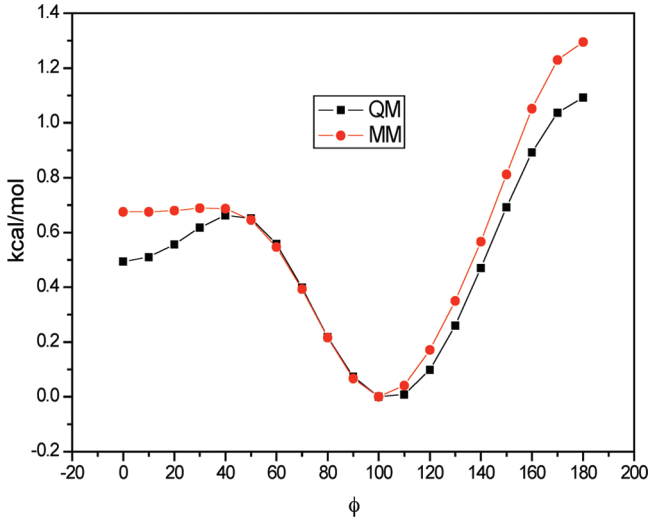

Figure 2. Comparison of the dihedral energy profiles involving the NR-CN2 bond (see Figure 1) in the [$C_n$mim] cation obtained from ab initio calculations (QM) and the optimized force field (MM).

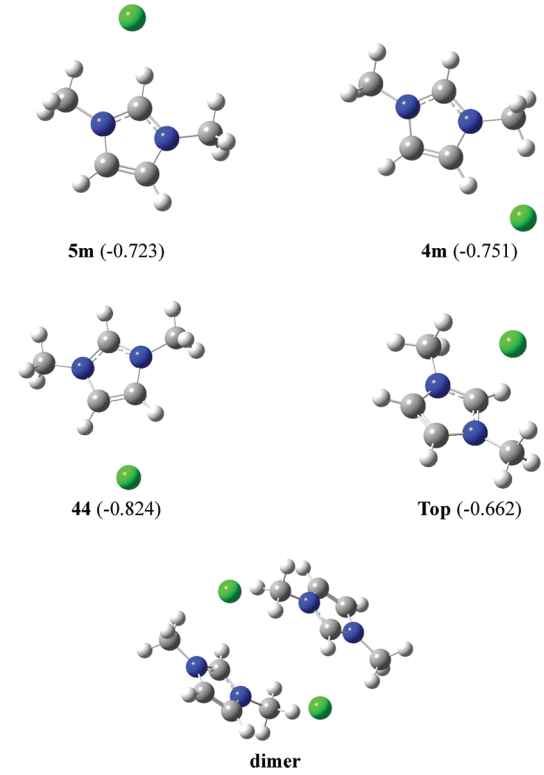

Figure 3. Four optimized isomers for the [C_1mim][Cl] ion pair and its dimers, obtained by ab initio calculation at the B3LYP/6-31+G(d,p) level. The charges on chloride are shown as the numbers in parentheses.

the same as in our previous work. These were determined by a compromise of XRD experiments and QM computations. The corresponding force constants were extracted from the recently developed general AMBER force field (GAFF),[68] which is slightly different from the constants used in our previous work. The parameters related to the united atoms came from amberff03_ua.[69] The coefficients for the dihedrals involving the bond NR-CN2 are completely refitted by a method described in section 2.1. Figure 2 shows good agreement between the ab initio calculation and the result obtained from the optimized force field. To decrease the computational costs, we carry out quantum chemical calculations of the torsion energy at the MP2/cc-pVTZ//B3LYP/6-31+G(d,p) level (see section 2.1) rather than at the MP4/6-311G(d,p)//MP2/6-31G* level used in AMBER−GAFF. However, the results showed that there is only a marginal difference between the two methods.

3.2. Atom Partial Charge Assignment. As mentioned in section 1, substantial improvement in the simulated dynamic properties can be made by a charge-fitting scheme in which the total charges on cations and anions are reduced to an absolute value smaller than 1*e*. Thus, the charge transfer and polarizability is accounted for in an effective way.

It is also well-known that the charge distribution is strongly dependent on the geometry of the molecule, the basis sets, the method used for ab initio calculations, and the charge fitting scheme. These uncertainties have to be addressed before one can use the absolute value of the charges directly. Important questions in optimizing the charges in a nonpolarizable force field are (1) how to determine the amount of charge transfer between the cations and anions and (2) how to get an average polarizability analogue to those in liquids. The recent work by Klähn et al.[55] provides a promising method in which a combined quantum mechanical/molecular mechanical (QM/MM) approach was used to obtain the charge distribution in the "actual" liquid for the guanidinium ILs. The total charges on the cation and anion were derived by QM/MM calculations, in which QM was used to treat six ion pairs, and MM was used to treat the surrounding 494 ion pairs, whereas the average polarizabilty was obtained by replacing the QM part with one cation or anion. It is noted, though, that the cost of this method is also very high; however, the method is much more effective than a fully ab initio MD simulation.

In this work, we used ab initio calculations of ion pair dimers to fit the atom partial charges by the RESP method (see section 2.1 for details). Fitting to the isolated ion pairs[18,28,54] has at least two drawbacks. The first is that charges fitted from different conformers are significantly different. Starting from 10 different initial configurations of ion pairs, we obtained 4 converged conformers for [C_1mim][Cl], as shown in Figure 3, and labeled as **5m** (chloride between H5 and methyl), **4m**, **44**, and **top**, respectively. The conformers are in plane except for **top**, consistent with previous findings.[58,70] The most stable conformer is **5m**, followed by **top**, which has a slightly higher energy (see Table 2). In fact, the difference in the relative energies of **5m** and **top** is very small, which will be reversed (see Table 2) when a different ab initio method is employed.[58,70] The fitted charges are highly dependent on the geometries of the conformers, that is, the position of chloride relative to the cation. It is difficult to get an averaged charge distribution from these conformers, even though the multiconformer RESP fitting can be performed. In Figure 4a, furthermore, the position of the first peak of H5−Cl RDFs obtained by ab initio MD is at ∼0.23 nm,[57,58] whereas none of the four isolated ion pair conformers gives a distance that agrees with this value, as can be seen from Table 1.

By contrast, the H5−Cl distance in the optimized ion pair dimer, 0.231 75 nm, is in good agreement with the averaged value obtained from ab initio MD. The value of the CR−H5−Cl angle, 136.7, is also consistent with the statistical analysis of ab initio MD trajectories[58] (see Figure 7 in ref 58). The second drawback of fitting using isolated cation−anion pairs is that the charge transfer is exaggerated in such ion pairs because every ion is actually coordinated by 5−6

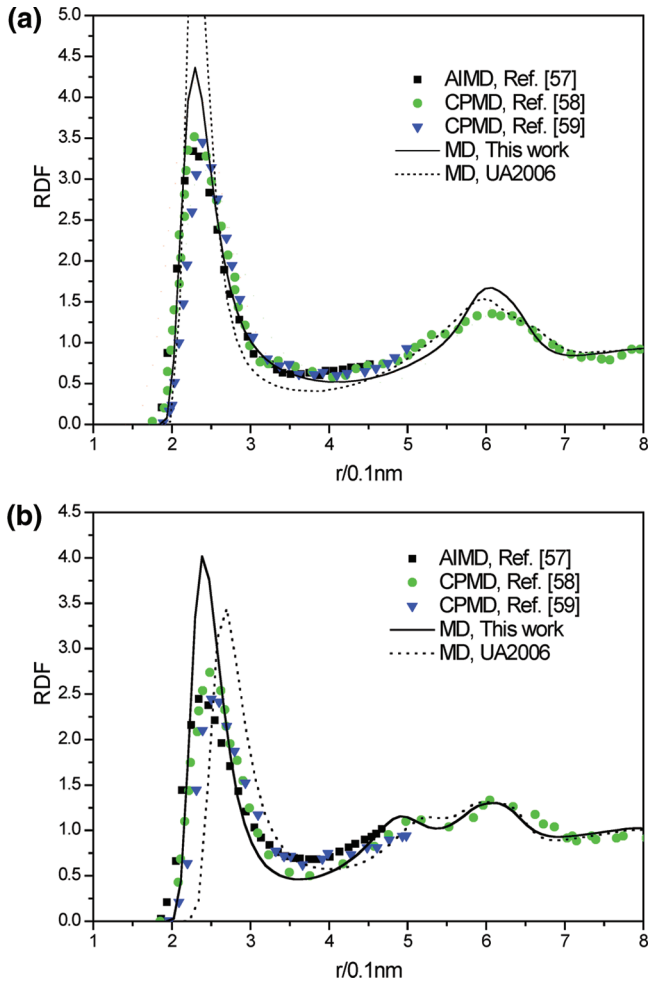

Figure 4. (a) Site−site radial distribution functions of H5−Cl in [C_1mim][Cl] by classical and ab inito MD simulations. Solid line, by force field in this work; dotted line, by force field in ref 20 (UA2006); squares, ab inito MD by Del Popolo et al.;[57] circles, CPMD by Buhl et al.;[58] triangles, CPMD by Bhargara and Balasubramanian.[59] (b) Site−site radial distribution functions of H4−Cl in [C_1mim][Cl] by classical and ab inito MD simulations. Solid line, by force field in this work; dotted line, by force field in ref 20 (UA2006); squares, ab inito MD by Del Popolo et al.;[57] circles, CPMD by Buhl et al.;[58] triangles, CPMD by Bhargara and Balasubramanian.[59]

counterions in a liquid, as was found by both classical MD[40,71] and ab initio MD.[57,58] Static quantum chemical calculations of linear chains up to nine ion pairs showed[70] that the average charge (absolute value) on chloride increased from 0.735 on the isolated ion pair to 0.814 on the linear nine ion pair chain, with an extrapolated value of 0.823 for an infinitely long chain. The absolute value of the charges on chloride obtained in this work are 0.723, 0.751, 0.824, 0.662, and 0.705 for the **5m**, **4m**, **44**, **top**, and **dimer** conformers, respectively. All of the values are smaller than 0.8 except for **44**. The structure of **44** is evidently seldom found in the liquid state (compare the geometric parameters in Table 1 and Figures 3 and 7 in ref 58). An averaged value of −0.75 was obtained by MPA over 20 snapshots taken between 3.0 and 5.0 ps from CPMD simulations.[58] For comparison, the charge was −0.79 in a force field optimized via a force-matching method,[41] as mentioned in section 1. Therefore, all the charges obtained for the dimer were scaled up from 0.705 to 0.80.

The results for [$C_n$mim][Cl] ($n \geq 2$) are very similar to those for [C_1mim][Cl]. The details for these ILs can be found in the Supporting Information. For ILs with longer chains ($n > 2$), the scheme of our previous work[20] was used. The charges on CH_2 and CH_3 united atoms in the longer chain were simply set to zero. To confirm the reasonability of this method, the ion pair dimer of [C_3mim][Cl] was optimized by ab initio calculations done at the same level as those done for [C_2mim][Cl]. The fitted charge on the end of the CT3 united atom is as small as −0.0263 (see Table S3 in the Supporting Information). Thus, neglect of the charges on longer chains will not lead to much difference in the force field.

Transferability is always a very important quality of any force field. A reasonable compromise was obtained by scaling of the RESP charges and neglecting the charges on longer alkyl chains. Extending the force field in this work to other ILs is in progress. The final set of charges can be found in Table S1 in the Supporting Information.

3.3. Lennard-Jones Parameters Adjustmentment. It is expected that a force field with scaled-down charges (<1) will give a lower liquid density if other parameters remain unchanged. Youngs et al. showed[41] that a reduction from 1.0 to 0.8 resulted in about a 5% decrease in the simulated density of [C_1mim][Cl]. Thus, additional adjustment of LJ parameters is necessary. The work of Köddermann et al.[51] also showed that a significant improvement of the force field for an IL could be achieved by optimizing LJ parameters.

Here, we have used the same strategy as that used in previous work[19] to adjust the LJ parameters. To maintain a good transferability of C and N atoms in well-established force field such as CHARMM and AMBER, only the LJ parameters for only two hydrogen atoms (H4 and H5) were adjusted. It is reported[72] that the adjustment of the LJ parameters for anions is an efficient way to improve the force field for ILs. We did not adjust the LJ parameters for the chloride anion because the parameters came from the well-developed and widely used Tosi−Fumi potential for molten salts.[73] In addition, it is unclear whether the parameters of the cation [$C_n$mim] are sufficient. Combinations of [$C_n$mim] and more anions are necessary to develop transferable force fields covering a large variety of ILs, a task that is beyond the scope of the present work.

TABLE 1: RESP Charges in |*e*|, Selected Angles in Degrees, and Distances in 0.1 nm, for Four Conformers of [C_1mim][Cl] Ion Pairs and Its Dimers, Calculated at the B3LYP/cc-pVTZ//B3LYP /6-31+(d,p) Level in This Work

	charges							angles[a]		distances[b]	
	H5	H4	CW	NA	CN3	CR	Cl	H5	H4	H5	H4
5m	0.115	0.184	−0.178	0.033	0.249	0.034	−0.723	160.0		1.9892	
4m	0.181	0.161	−0.094	0.031	0.246	−0.117	−0.751		150.2		2.1509
44	0.267	0.168	−0.109	0.202	0.245	−0.455	−0.824		112.2		2.5460
top	0.179	0.207	−0.170	−0.068	0.260	0.026	−0.662	79.2		2.6476	
dimer	0.137	0.191	−0.162	0.034	0.222	−0.003	−0.705	136.7	110.4	2.3175	2.9702

[a] Angles of Cl−H5(H4)−CR(CW). [b] Distances of Cl−H5(H4).

TABLE 2: Interaction Energies (E_I) and the Relative Values (ΔE_I) in kcal/mol for Four Conformers of [C$_1$mim][Cl] Ion Pairs Calculated at the B3LYP/cc-pVTZ//B3LYP/6-31+G(d,p) Level (QM) and Force Field (MM) in This Work and by Various Ab Initio Calculations (QM) in the Literature

	this work			literature (QM, ref 70[a])							
	E_I	ΔE_I		E_I				ΔE_I			
	MM	MM	QM	HF	BP86	B3LYP	MP2	HF	BP86	B3LYP	MP2
5m	−53.9	0	0	−103.6	−107.5	−96.7	−89.0	0.0	0.0	0.0	0.0
4m	−50.5	3.5	8.3	−83.0	−90.5	−88.2	−81.0	20.6	17.0	8.5	7.9
44	−47.1	6.9	15.6	−75.5	−83.1	−80.7	−76.0	28.1	24.5	16.0	12.9
top	−54.6	−0.65	0.43	−86.7	−102.2	−97.8	−91.9	16.9	5.4	−1.1	−3.0

[a] The data in ref 70 were obtained with the TZVP basis set, except HF, which is calculated with the 3-21G basis set.

TABLE 3: Near Distances in 0.1 nm between Chloride and Various Atoms (X) on the [C$_1$mim] Cation, Optimized by Ab Initio (QM) and Force Field (MM) in This Work

	X	QM	MM	dr
5m	H5	1.9891	2.2662	0.2771
	CR	3.0703	3.2266	0.1563
	NA	3.7423	3.7591	0.0168
	CN3	3.5952	3.5191	−0.0761
4m	H4	2.1517	2.1730	0.0213
	CW	3.1721	3.1709	−0.0012
	NA	3.6816	3.7210	0.0393
	CN3	3.3821	3.4835	0.1014
44	H4	2.5465	2.6175	0.0710
	H4	2.5451	2.6170	0.0719
	CW	3.1214	3.1665	0.0451
top	NA	3.2265	3.7970	0.5706
	CR	2.6632	3.0658	0.4026
	CW	3.9044	4.8178	0.9133
	H5	2.6469	2.3461	−0.3008
	CN3	3.5517	4.0175	0.4658

The conformers of isolated ion pairs were used to adjust the LJ parameters of H5 and H4 on the [C$_n$mim] cation, and others were kept the same as in our previous work.[20] As is shown in Table 3, most of the deviations of the distances between the chloride anion and the atoms on the cation were within 0.01 nm, although the geometries of **top** actually could not be well-reproduced by the force field.

The final optimized parameters can be found in Table S1 in the Supporting Information.

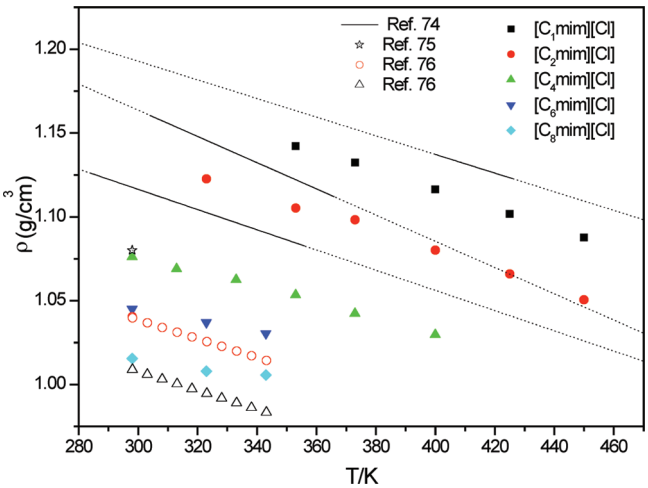

Figure 5. Liquids densities of [C$_n$mim][Cl] as a function of temperature. Solid symbols, predicted by the force field in this work; open symbols, experimental data (refs 75 and 76); solid lines, linear fitting of experimental data (ref 74) within the temperature range measured; dotted line, extrapolation of the linear fitting out of the temperature range measured.

4. Results and Discussion

4.1. Liquid Densities and Heats of Vaporization. The simulated liquid densities obtained in this work were in good agreement with those measured experimentally[74−76] (see Figure 5), even though we used a simple method (see section 3.2) to extrapolate the force field to [C$_n$mim][Cl] when $n > 2$. This is not surprising because we adjusted the LJ parameters of H4

TABLE 4: Simulated Densities (ρ_{sim}) in g/cm^3, Heats of Vaporization (ΔH^{vap}) in kcal/mol, Cohesive Energies (c) in J/cm^3, and Self-Diffusion Coefficients (D) in 10^{-12}m^2/s, of [C$_n$mim][Cl] by the Force Fields Proposed in This Work and Ref 20 (in parentheses)

T/K	ρ_{sim}	ρ_{exp}	ΔH^{vap}	c	D_+	D_-
			[C$_1$mim]			
353	1.142	1.16	150	1289	22.6	11.8
373	1.132 (1.171)	1.15	148 (200)	1262 (1762)	45.2	34.5
400	1.116 (1.162)	1.14	145 (198)	1222 (1731)	145 (7.7)	125 (4.9)
425	1.102 (1.148)	1.12	144 (196)	1199 (1694)	239 (18)	206 (13)
450	1.088 (1.136)	1.11	142 (194)	1162 (1663)	465 (39)	377 (28)
			[C$_2$mim]			
323	1.1226	1.15	152	1166	5.2[a]	4.1[a]
353	1.1053	1.12	150	1131	26	18
373	1.0983	1.11	148	1109	56	40
400	1.0802 (1.105)	1.09	146 (210)	1073 (1585)	132 (8.2)	112 (5.4)
425	1.0659 (1.097)	1.07	144 (209)	1045 (1576)	301 (20)	226 (17)
450	1.0505 (1.083)	1.05	141 (207)	1010 (1527)	407 (75)	345 (71)
			[C$_4$mim]			
298	1.0761	1.08	162	996	0.22[b]	0.18[b]
313	1.0689		161	984	1.22[a]	0.95[a]
333	1.0625		160	971	1.46[b]	1.38[b]
353	1.0533		159	956	3.9[a]	3.2[a]
373	1.0422		156	933	11.2[b]	9.9[b]
400	1.0296		154	910	43.4	34.0
			[C$_6$mim]			
298	1.0450	1.039	173	890	0.46[a]	0.69[a]
323	1.0371	1.025	171	875	1.5[a]	1.1[a]
343	1.0305	1.014	170	866	4.9	3.9
			[C$_8$mim]			
298	1.0154	1.009	184	816	0.39[a]	0.42[a]
323	1.0079	0.995	182	800	0.53[a]	0.43[a]
343	1.0056	0.983	181	788	1.29[a]	1.82[a]

[a] These values of self-diffusion coefficients are fitted far from the diffusion region. Thus, these values are not the "true" numbers of the self-diffusion coefficients. See discussion in section 3.2 for details. [b] Values were determined fitting the slope of MSD between 4 and 6 ns.

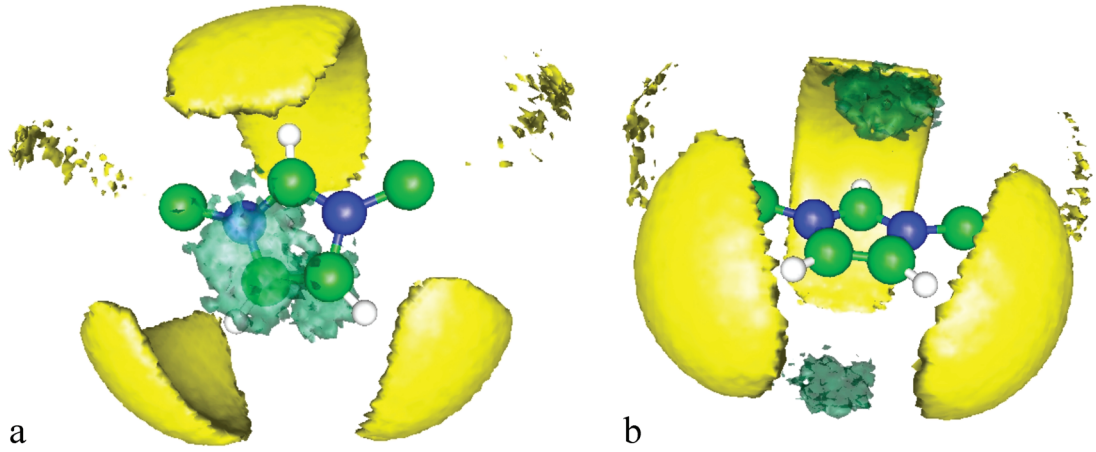

Figure 6. Three-dimensional probability distributions of chloride (yellow) and CR on cations (green) around cations in ionic liquid [C_1mim][C1]. Density levels correspond to 5 and 3 times the bulk density for anions and cations, respectively.

and H5 by the ab initio optimized geometries of isolated ion pairs, which has been shown to give better liquid density predictions.[19]

The heat of vaporization was estimated by the difference between the total potential energies of an IL in the liquid and gas phases:

$$\Delta H^{vap} = U^{gas} - U^{liq} + RT \quad (2)$$

The potential energy in the gas phase was obtained from simulations of isolated ion pairs at the same temperature without long-range corrections. The cohesive energy is defined as

$$c = \Delta H^{vap}/V_m \quad (3)$$

where V_m is the molar volume.

The simulated heats of vaporization and cohesive energies are listed in Table 4, together with some results obtained using our previous UA force field (referred as UA2006).[20] The heats of vaporization obtained in this work are more than 30% lower than those obtained using the UA 2006 force field. Unfortunately, the experimental data for the heat of vaporization are not available for most of the ILs examined. An estimated heat of vaporization of 155 kJ/mol was obtained by ab initio MD for [C_1mim][Cl] at 450K,[57] which is 8% higher than the value of 142 kJ/mol in this work.

4.2. Radial Distribution Functions and Three-Dimensional Distributions. Usually, the liquid structure is described by site−site radial distribution functions (RDFs). Information from NMR and IR experiments indicate that for imidazolium ILs, the most noticeable interactions are those between the acid hydrogens on the imidazolium ring (H5 and H4 in Figure 1) and anions. Figure 4a and b show the RDFs of H5−Cl and H4−Cl in liquid [C_1mim][Cl], respectively. The results of ab initio MD (AIMD or CPMD)[57−59] are also shown for comparisons.

The RDF of H5−Cl exhibits a sharp peak at 0.22 nm and a second broad one at ~0.6 nm for the both the UA2006 force field and the one developed in this work. The RDFs obtained with both of these force fields show good agreement with that obtained from AIMD. The intensity of the first peak was as high as 6.3 using the UA2006 force field. By contrast, the intensity of this peak decreased to 4.2 when the force field developed here was used, placing it much closer to the value obtained by AIMD, 3.5. The position of the first peak in the H4−Cl RDF was quite different for the two force fields: 0.22 nm for the force field developed in this study and 0.27 nm for the UA2006 force field. The force field developed here showed a significant improvement on the structure of liquid [C_1mim][Cl] relative to that obtained using the UA2006 force field; however, both force fields showed an overstructuring of the liquids, as indicated by the intensities of the first peak. It seems that reducing the total charges to ±0.8e, although yielding a significant

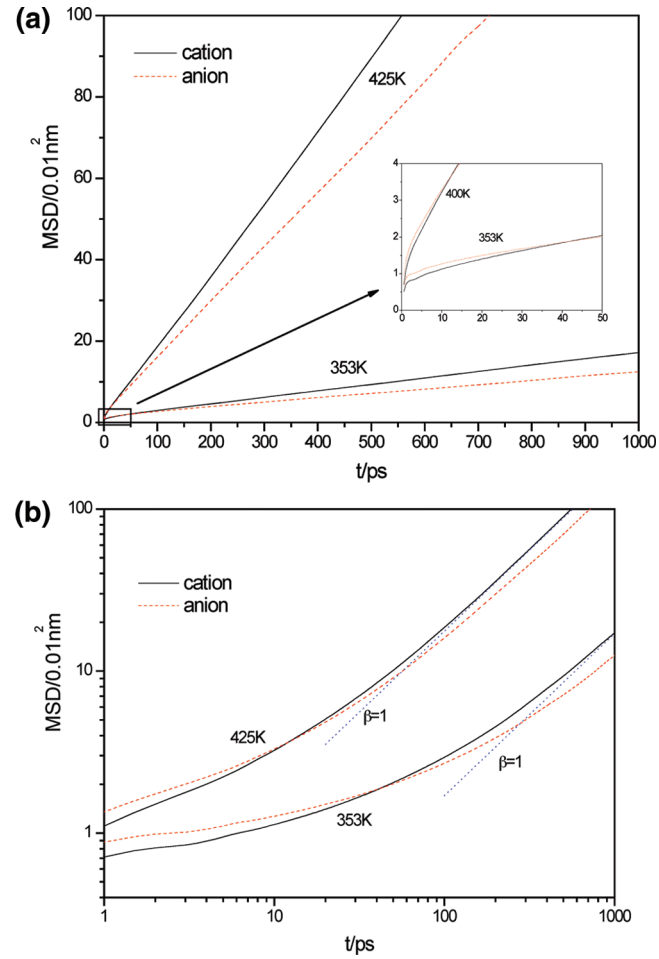

Figure 7. (a) Mean square displacements (MSDs) of cations and anions in [C_2mim][Cl] at temperatures of 353 and 425 K calculated by 2 ns MD trajectories. The inset figure shows the short-time MSD within 50 ps. (b) The same as Figure 8, but in log−log scale. The slope of 1 (β = 1) is shown as a blue dotted line.

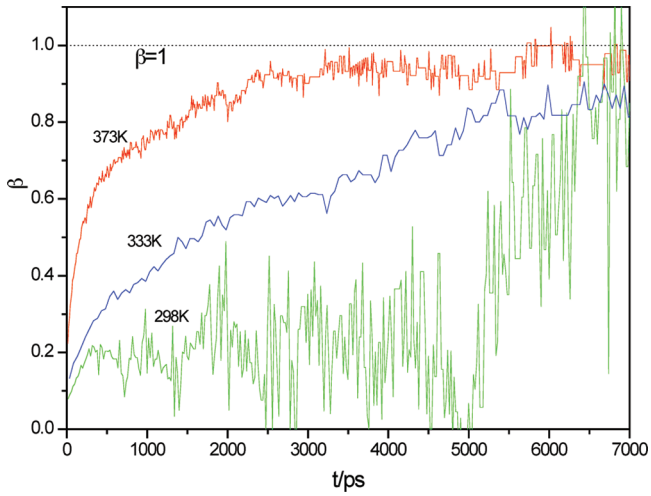

Figure 8. The values of β (defined in section 3.2) for [C$_4$mim][Cl] as a function of time, at 373, 333, and 298 K.

improvement, is insufficient to give close agreement with the results from AIMD. It has been reported that reducing the charges to between ±0.6 and 0.7e gives the best agreement with AIMD.[41]

The three-dimensional distribution around a central molecule can be described with an angular distribution, using a visualization packages such as gOpenMol. Figure 6 shows that there are three major regions where chloride anions are most likely to be found around a cation in liquid [C$_1$mim][Cl]. Each of these zones is near the ring hydrogens in the imidazolium cation. This finding agrees very well qualitatively with that obtained from AIMD simulations.[57−59] As discussed in section 3.2, none of the four conformers (**5m**, **4m**, **top**, and **44**) of isolated ion pairs coincides with the distribution regions shown in Figure 6. By contrast, the position of chloride anions in the **dimer** conformer is consistent with that found in the liquid state (see atom coordinations in the Supporting Information). Consequently, the **dimer** conformer provides a more reasonable basis for fitting charges than do isolated ion pairs.

4.3. Self-Diffusion Coefficients. Table 4 shows the simulated self-diffusion coefficients for the cations and anions of [C$_n$mim][Cl] determined from the Einstein relation,

$$D_i = \frac{1}{6}\lim_{t\to\infty}\frac{\mathrm{d}}{\mathrm{d}t}\langle[\vec{r}_i(t) - \vec{r}_i(0)]^2\rangle = \frac{1}{6}\lim_{t\to\infty}\frac{\mathrm{d}\Delta r_i^2}{\mathrm{d}t} \qquad (4)$$

where the quantity in ⟨...⟩ is the ensemble-averaged mean square displacement (MSD) of the center-of-mass of the cations or anions. One nanosecond MSDs were calculated by using 2 ns MD trajectories with time increments of 0.5 ps in each case, except for a few cases discussed below. The typical MSDs are shown in Figure 7a for [C$_2$mim][Cl] determined for temperatures of 353 and 425 K.

The eq 4 is valid only when true diffusive motion is observed. It is well-known that ILs show very slow dynamics, with self-diffusion coefficients on the order of 10^{-11} m^2/s. Therefore it is important to know how long the simulation needs to be continued to compute the MSD and which regime should be used to fit the self-diffusion coefficient. Cadena et al. have argued[48] that self-coefficients determined using MSDs calculated for too short time usually led to an overestimation of the correct values.

In Figure 7a, it appears that the MSDs become linear after a few picoseconds. However, as shown in Figure 7b, reploting the results on a log−log scale shows this not to be true. At 425 K, the value of $\beta(t) = (\mathrm{d}\log\Delta r_i^2(t))/(\mathrm{d}\log t)$ approaches 1.0 when t is larger than 200 ps, whereas the motion at 353 K

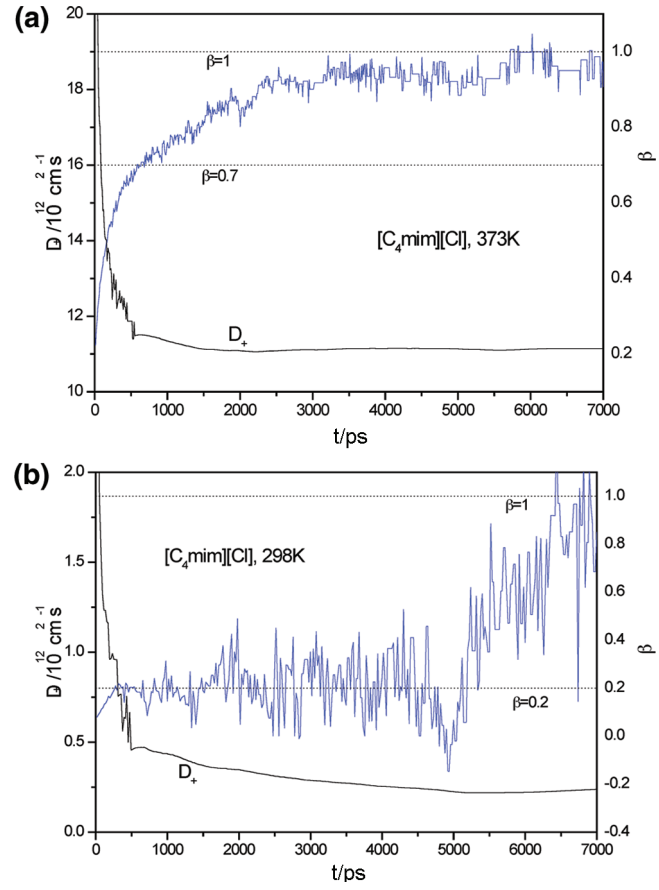

Figure 9. (a) The self-diffusion coefficients of [C$_4$mim][Cl] at 373 K by fitting different time spans of MSD. The values of β are shown in the blue line. (b) The self-diffusion coefficients of [C$_4$mim][Cl] at 298 K, by fitting different time spans of MSD. The values of β are shown in the blue line.

remains in the sublinear regime, which is characterized by $\beta(t) < 1$, even when $t > 1$ ns.

To obtain longer time MSDs, simulations longer than 15 ns were carried out for [C$_4$mim][Cl] at 298, 333, and 373 K. Values of $\beta(t)$ for the cation are shown in Figure 8.

Figure 9a shows the self-diffusion coefficients at 373 K as a function of the fitting time regimes. Although $\beta(t)$ did not approach 1.0 until 4 ns, the fitting values of D_+ were essentially unchanged after 1 ns. The value obtained by fitting the slope between 500 and 1000 ps ($\beta \approx 0.7$) was 11.4, as compared with the value of 11.2 obtained by fitting between 4 and 6 ns, a deviation of only 2%.

At 298 K, the values of β fluctuated strongly around 0.2 when $t < 5$ ns, then jumped to 0.8 for $t = 6$ ns, as shown in Figure 9b. The value of the self-diffusion coefficients decreased from 0.46×10^{-11} m^2/s at 500 ps to 0.22×10^{-11} m^2/s at 6 ns. Consequently, the value obtained between 500 and 1000 ps overestimated the correct value by more than 100%.

The preceding discussion demonstrates that the value of β must be determined to ensure that MSDs give the correct self-diffusion coefficient. Our work has shown that determination of the self-diffusion coefficient when β is larger than 0.7 does not lead to a significant overestimation of the self-diffusion coefficient. For ILs with self-diffusion coefficients $<10^{-11}$ m^2/s, 2 ns simulations are insufficient.

At 425 K, the present force field gives values of self-diffusion coefficients of cations and anions in [C$_1$mim][Cl] of 239×10^{-12}

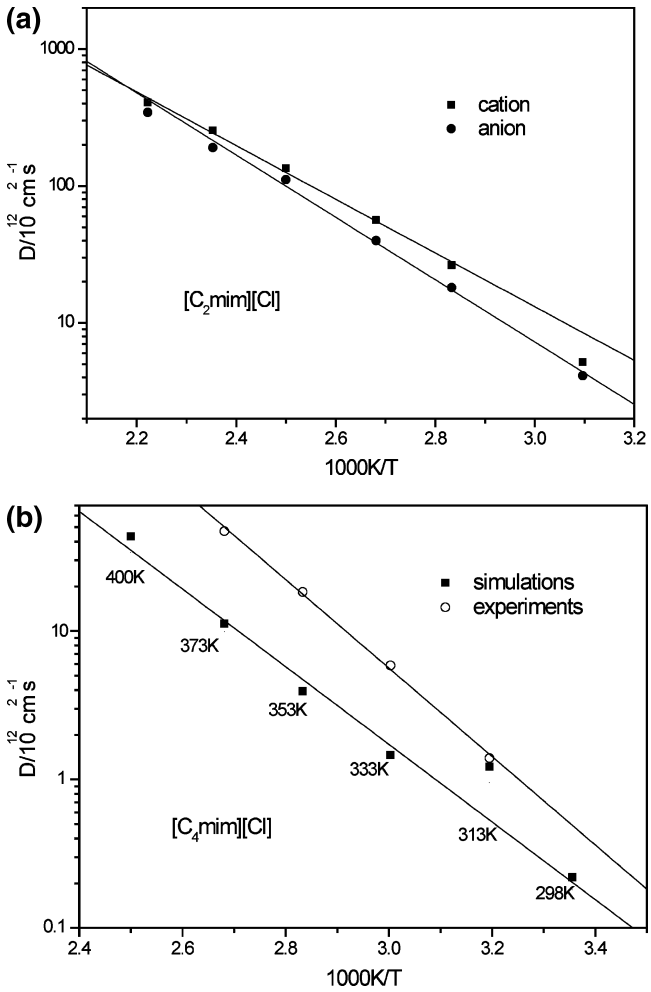

Figure 10. (a) Temperature dependence of self-diffusion coefficients of cations and anions in [C_2mim][Cl], as predicted by molecular simulations with the force field in this work. The lines are linear fits of the curves. (b) Temperature dependence of self-diffusion coefficients of cations in [C_4mim][Cl], as predicted by molecular simulations with the force field in this work (solid square), compared with experimental measurements (open circle) by Remsing et al.[77] The lines are linear fits of the curves.

and 206 × 10^{-12} m^2/s, respectively, as compared to 18 × 10^{-12} and 13 × 10^{-12} m^2/s obtained from our previously developed UA2006 force field,[20] and values of 31 × 10^{-12} and 22 × 10^{-12} m^2/s[71] obtained using the all-atom force field developed by Lopes et al.[14] Consequently, the force field developed in this study gives a substantial improvement relative to results obtained using other nonpolarizable force fields.[14,20]

The temperature dependence of the self-diffusion coefficients of the cations and anions of [C_2mim][Cl] are shown in Figure 10. Both self-diffusion coefficients can be expressed in the form of an Arrhenius equation:[46]

$$D_i = D_{i,0} \exp\left(-\frac{E_D^a}{RT}\right) \tag{5}$$

where E_D^a is the apparent activation energy. From the slope of the plot of $\log(D_i)$ versus $1/T$, we obtained the values 16.3 and 18.9 kJ/mol for the cations and anions, respectively.

Recently, Remsing et al.[77] measured the self-diffusion coefficients of cations in [C_4mim][Cl] by the ^{1}H pulsed field gradient stimulated echo method. Figure 10b compares the

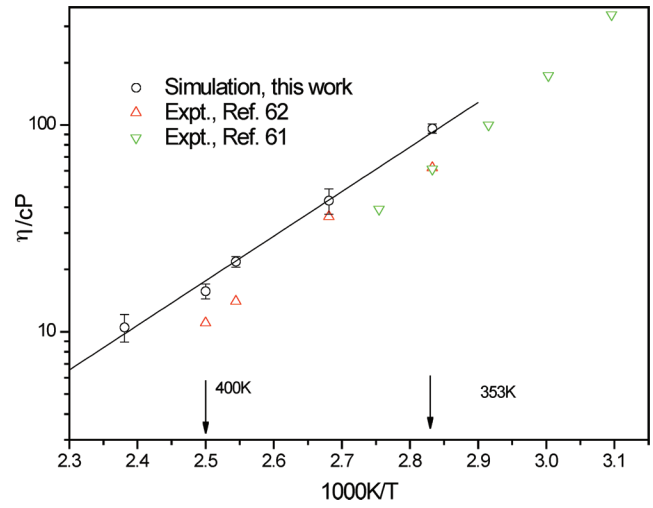

Figure 11. Temperature dependence of the viscosity of [C_2mim][Cl]. Circles, predicted by the force field in this work; up triangles, experimental measurements by Chen et al.;[62] down triangles, experimental measurements by Seddon et al.[61]

simulated results in this work and the measurements. The simulated self-diffusion coefficients are about 1/4 those measured experimentally, whereas the experimentally determined apparent activation energies agree well with those determined by simulation.

4.4. Viscosities. The zero-shear viscosity was calculated via equilibrium MD using the Green−Kubo (GK) formula,[78,79]

$$\eta = \frac{V}{10k_BT}\int_0^\infty \left\langle \sum_{\alpha\beta} P_{\alpha\beta}(0)\, P_{\alpha\beta}(t) \right\rangle \mathrm{d}t \tag{6}$$

$P_{\alpha\beta}$ is the symmetrized traceless portion of the stress tensor ($\sigma_{\alpha\beta}$) and is defined as

$$P_{\alpha\beta} = \frac{1}{2}(\sigma_{\alpha\beta} + \sigma_{\beta\alpha}) - \frac{1}{3}\delta_{\alpha\beta}\left(\sum_r \sigma_{\gamma\gamma}\right) \tag{7}$$

where $\delta_{\alpha\beta}$ is the Kronecker delta and $\delta_{\alpha\beta} = 0$ when $\alpha \neq \beta$. The accuracy and applicability of pressure fluctuation-based equilibrium methods (such as the GK formula or the Einstein relation) have been discussed in ref 80. Note that all nine components of the pressure tensor were used in eq 6 to improve the statistics. This is important, since viscosity is a collective property of the entire system and the accuracy of viscosity calculations cannot be improved by averaging over all particles in the system. For this reason, it is desirable to maximize the use of all available information contained in the simulation. Consequently, pressure tensor information was recorded at every time step and a trajectory of 20 ns was used to compute the viscosity. In computing the time correlation function, we used the multiple-time origin average method to improve the statistics. The block-averaging method was used to obtain the viscosity and estimate the corresponding error bars. Figure S5 of the Supporting Information illustrates a typical viscosity curve for [C_2mim][Cl] at 353 K. The viscosity of 96 ± 5 cP was obtained by averaging over t = 2−4 ns.

The viscosities predicted by the force filed developed in this work were about 50% higher than those measured experimentally.[61,62] The result will most likely improve in a force

field in which the polarizability is considered explicitly.[32] Figure 11 shows an Arrhenius plot. Despite the discrepancy between the experimentally measured and the simulated viscosities, both give similar temperature dependences. By fitting the slopes of $\log(\eta)$ versus $1/T$ in Figure 11, an apparent activation energy of 17.6 kJ/mol was obtained, which is in good agreement with the experimental value of 22.8 kJ/mol.

The force field introduced in this work gives a much improved value of viscosity, as compared with that obtained using the UA2006 force field[20] and other nonpolarizable force fields that do not utilize reduced charges. For example, the new force field gives a viscosity at 400 K of 15.7 cP, in contrast to 450 cP obtained using the UA2006 force field, and 200 cP[46] obtained using the UA force field developed by Kim et al.[49]

5. Conclusions

A cost-effective united-atom force field for 1-alkyl-3-methyl-imidazolium chloride ([$C_n$mim][Cl], $n = 1, 2, 4, 6, 8$) has been developed that uses effective atom partial charges to account for the overall effects of polarization. These charges were determined by fitting the electrostatic potential surface (ESP) of ion pair dimers. Molecular dynamics (MD) simulations were performed over a wide range of temperatures to validate the force field. The simulated liquid densities are in good agreement with those measured experimentally. The site−site radial distribution functions between the hydrogen atoms on the imidazolium ring and the chloride anion agree well with those determined by ab initio molecular dynamics. The self-diffusion coefficients of the cations and anions were ∼1 order of magnitude larger than those determined using previously developed force fields. Although shear viscosities calculated from equilibrium MD simulations using the Green−Kubo formula were ∼50% larger than those measured experimentally, the values are significantly closer to the experimental values than those obtained from simulations made with nonpolarizable force fields but no reduction in the charges.

Acknowledgment. Financial support of B.P. through the Energy Biosciences Institute (EBI) is gratefully acknowledged. We also thank Dr. Patricia Hunt at Imperial College London and Dr. Seiji Tsuzuki at the National Institute of Advanced Industrial Science and Technology (AIST, Japan) for the friendly discussion on charge-fitting by ab initio results.

Supporting Information Available: All the parameters of the force fields for [$C_n$mim][Cl] can be found in Table S1. The atom coordinates in the optimized geometries of monomers and dimers of [C_1mim][Cl] and [C_2mim][Cl] are given in Table S2. Figures S1 and S2 give results for [C_2mim][Cl] similar to those discussed in section 3 for [C_1mim][Cl]. Figures S3 and S4 show typical distributions of the counterions around the central anion and cation. Figure S5 gives a typical integral of the correlation function used to estimate the viscosity. This material is available free of charge via the Internet at http://pubs.acs.org.

References and Notes

(1) Welton, T. *Chem. Rev.* **1999**, *99* (8), 2071–2083.
(2) Blanchard, L. A.; Hancu, D.; Beckman, E. J.; Brennecke, J. F. *Nature* **1999**, *399* (6731), 28–29.
(3) Lu, W.; Fadeev, A. G.; Qi, B. H.; Smela, E.; Mattes, B. R.; Ding, J.; Spinks, G. M.; Mazurkiewicz, J.; Zhou, D. Z.; Wallace, G. G.; MacFarlane, D. R.; Forsyth, S. A.; Forsyth, M. *Science* **2002**, *297* (5583), 983–987.
(4) Kuang, D.; Brillet, J.; Chen, P.; Takata, M.; Uchida, S.; Miura, H.; Sumioka, K.; Zakeeruddin, S. M.; Gratzel, M. *ACS Nano* **2008**, *2* (6), 1113–1116.
(5) Soukup-Hein, R. J.; Warnke, M. M.; Armstrong, D. W. *Annu. Rev. Anal. Chem.* **2009**, *2*, 145–168.
(6) Freemantle, M. *Chem. Eng. News* **2007**, *85* (1), 23–26.
(7) Weingaertner, H. *Angew. Chem., Int. Ed.* **2008**, *47* (4), 654–670.
(8) Yang, Y. L.; Kou, Y. *Chem. Commun.* **2004**, (2), 226–227.
(9) Umebayashi, Y.; Mitsugi, T.; Fujii, K.; Seki, S.; Chiba, K.; Yamamoto, H.; Lopes, J. N. C.; Padua, A. A. H.; Takeuchi, M.; Kanzaki, R.; Ishiguro, S. *J. Phys. Chem. B* **2009**, *113* (13), 4338–4346.
(10) Hunger, J.; Stoppa, A.; Schrodle, S.; Hefter, G.; Buchner, R. *ChemPhysChem* **2009**, *10* (4), 723–733.
(11) Xiao, D.; Hines, L. G.; Li, S. F.; Bartsch, R. A.; Quitevis, E. L.; Russina, O.; Triolo, A. *J. Phys. Chem. B* **2009**, *113* (18), 6426–6433.
(12) Mele, A.; Tran, C. D.; Lacerda, S. H. D. *Angew. Chem., Int. Ed.* **2003**, *42* (36), 4364–4366.
(13) Hardacre, C.; Holbrey, J. D.; Nieuwenhuyzen, M.; Youngs, T. G. A. *Acc. Chem. Res.* **2007**, *40* (11), 1146–1155.
(14) Lopes, J. N. C.; Deschamps, J.; Padua, A. A. H. *J. Phys. Chem. B* **2004**, *108* (6), 2038–2047.
(15) Lopes, J. N. C.; Padua, A. A. H.; Shimizu, K. *J. Phys. Chem. B* **2008**, *112* (16), 5039–5046.
(16) Lopes, J. N. C.; Padua, A. A. H. *J. Phys. Chem. B* **2006**, *110* (39), 19586–19592.
(17) Lopes, J. N. C.; Padua, A. A. H. *J. Phys. Chem. B* **2004**, *108* (43), 16893–16898.
(18) Lee, S. U.; Jung, J.; Han, Y. K. *Chem. Phys. Lett.* **2005**, *406* (4−6), 332–340.
(19) Liu, Z. P.; Huang, S. P.; Wang, W. C. *J. Phys. Chem. B* **2004**, *108* (34), 12978–12989.
(20) Liu, Z. P.; Wu, X. P.; Wang, W. C. *Phys. Chem. Chem. Phys.* **2006**, *8* (9), 1096–1104.
(21) Liu, X. M.; Zhang, S. J.; Zhou, G. H.; Wu, G. W.; Yuan, X. L.; Yao, X. Q. *J. Phys. Chem. B* **2006**, *110* (24), 12062–12071.
(22) Wang, Y.; Pan, H.; Li, H.; Wang, C. *J. Phys. Chem. B* **2007**, *111* (35), 10461–10467.
(23) Cadena, C.; Maginn, E. J. *J. Phys. Chem. B* **2006**, *110* (36), 18026–18039.
(24) Sambasivarao, S. V.; Acevedo, O. *J. Chem. Theory Comput.* **2009**, *5* (4), 1038–1050.
(25) Zhang, X. C.; Huo, F.; Liu, Z. P.; Wang, W. C.; Shi, W.; Maginn, E. J. *J. Phys. Chem. B* **2009**, *113* (21), 7591–7598.
(26) Zhou, G. H.; Liu, X. M.; Zhang, S. J.; Yu, G. G.; He, H. Y. *J. Phys. Chem. B* **2007**, *111* (25), 7078–7084.
(27) Urahata, S. M.; Ribeiro, M. C. C. *J. Chem. Phys.* **2004**, *120* (4), 1855–1863.
(28) Morrow, T. I.; Maginn, E. J. *J. Phys. Chem. B* **2002**, *106* (49), 12807–12813.
(29) Hanke, C. G.; Price, S. L.; Lynden-Bell, R. M. *Mol. Phys.* **2001**, *99* (10), 801–809.
(30) Schröder, C.; Steinhauser, O. *J. Chem. Phys.* **2008**, *128* (22), 224503.
(31) Halgren, T. A.; Damm, W. *Curr. Opin. Struct. Biol.* **2001**, *11* (2), 236–242.
(32) Yan, T. Y.; Burnham, C. J.; Del Popolo, M. G.; Voth, G. A. *J. Phys. Chem. B* **2004**, *108* (32), 11877–11881.
(33) Borodin, O.; Smith, G. D. *J. Phys. Chem. B* **2006**, *110* (23), 11481–11490.
(34) Hu, Z. H.; Huang, X. H.; Annapureddy, H. V. R.; Margulis, C. J. *J. Phys. Chem. B* **2008**, *112* (26), 7837–7849.
(35) Borodin, O.; Smith, G. D.; Kim, H. *J. Phys. Chem. B* **2009**, *113* (14), 4771–4774.
(36) Chang, T. M.; Dang, L. X. *J. Phys. Chem. A* **2009**, *113* (10), 2127–2135.
(37) Picalek, J.; Minofar, B.; Kolafa, J.; Jungwirth, P. *Phys. Chem. Chem. Phys.* **2008**, *10* (37), 5765–5775.
(38) Wu, Y. J.; Tepper, H. L.; Voth, G. A. *J. Chem. Phys.* **2006**, *124* (2), 12.
(39) Hunt, P. A. *Mol. Simul.* **2006**, *32* (1), 1–10.
(40) Youngs, T. G. A.; Del Popolo, M. G.; Kohanoff, J. *J. Phys. Chem. B* **2006**, *110* (11), 5697–5707.
(41) Youngs, T. G. A.; Hardacre, C. *ChemPhysChem* **2008**, *9* (11), 1548–1558.
(42) Picalek, J.; Kolafa, J. *J. Mol. Liq.* **2007**, *134* (1−3), 29–33.
(43) Zhao, W.; Eslami, H.; Cavalcanti, W. L.; Muller-Plathe, F. *Z. Phys. Chemie-Int. J. Res. Phys. Chem. Chem. Phys.* **2007**, *221* (11−12), 1647–1662.
(44) Kowsari, M. H.; Alavi, S.; Ashrafizaadeh, M.; Najafi, B. *J. Chem. Phys.* **2008**, *129* (22), 224508.
(45) Dommert, F.; Schmidt, J.; Qiao, B. F.; Zhao, Y. Y.; Krekeler, C.; Delle Site, L.; Berger, R.; Holm, C. *J. Chem. Phys.* **2008**, *129* (22), 224501.

(46) Rey-Castro, C.; Vega, L. F. *J. Phys. Chem. B* **2006**, *110* (29), 14426–14435.
(47) Rey-Castro, C.; Tormo, A. L.; Vega, L. F. *Fluid Phase Equilib.* **2007**, *256* (1−2), 62–69.
(48) Cadena, C.; Zhao, Q.; Snurr, R. Q.; Maginn, E. J. *J. Phys. Chem. B* **2006**, *110* (6), 2821–2832.
(49) Shim, Y.; Choi, M. Y.; Kim, H. J. *J. Chem. Phys.* **2005**, *122* (4), 044511.
(50) Bhargava, B. L.; Balasubramanian, S. *J. Chem. Phys.* **2007**, *127* (23), 234503.
(51) Koddermann, T.; Paschek, D.; Ludwig, R. *ChemPhysChem* **2007**, *8* (17), 2464–2470.
(52) Koddermann, T.; Fumino, K.; Ludwig, R.; Lopes, J. N. C.; Padua, A. A. H. *ChemPhysChem* **2009**, *10* (8), 1181–1186.
(53) Wei, Z.; Leroy, F.; Balasubramanian, S.; Muller-Plathe, F. *J. Phys. Chem. B* **2008**, *112* (27), 8129–8133.
(54) Logothetit, G. E.; Ramos, J.; Economou, I. G. *J. Phys. Chem. B* **2009**, *113* (20), 7211–7224.
(55) Klahn, M.; Seduraman, A.; Wu, P. *J. Phys. Chem. B* **2008**, *112* (35), 10989–11004.
(56) Bhargava, B. L.; Balasubramanian, S. *J. Phys. Chem. B* **2007**, *111* (17), 4477–4487.
(57) Del Popolo, M. G.; Lynden-Bell, R. M.; Kohanoff, J. *J. Phys. Chem. B* **2005**, *109* (12), 5895–5902.
(58) Buhl, M.; Chaumont, A.; Schurhammer, R.; Wipff, G. *J. Phys. Chem. B* **2005**, *109* (39), 18591–18599.
(59) Bhargava, B. L.; Balasubramanian, S. *Chem. Phys. Lett.* **2006**, *417* (4−6), 486–491.
(60) Swatloski, R. P.; Spear, S. K.; Holbrey, J. D.; Rogers, R. D. *J. Am. Chem. Soc.* **2002**, *124* (18), 4974–4975.
(61) Seddon, K. R.; Stark, A.; Tepper, M. J. Viscosity and Density of 1-Alkyl-3-methylimidazolium Ionic Liquids. In *Clean Solvents: Alternative Media for Chemical Reactions and Processing*; Abraham, M. A., Moens, L., Eds.; American Chemical Society: Washington, DC, 2002; p 34.
(62) Chen, T.; Chidambaram, M.; Liu, Z.; Smit, B.; Bell, A. T. *J. Phys. Chem. B* **2009**, submmited.
(63) Frisch, M. J.; Trucks, G. W.; Schlegel, H. B.; Scuseria, G. E.; Robb, M. A.; Cheeseman, J. R.; Montgomery, J. A., Jr.; Vreven, T.; Kudin, K. N.; Burant, J. C.; Millam, J. M.; Iyengar, S. S.; Tomasi, J.; Barone, V.; Mennucci, B.; Cossi, M.; Scalmani, G.; Rega, N.; Petersson, G. A.; Nakatsuji, H.; Hada, M.; Ehara, M.; Toyota, K.; Fukuda, R.; Hasegawa, J.; Ishida, M.; Nakajima, T.; Honda, Y.; Kitao, O.; Nakai, H.; Klene, M.; Li, X.; Knox, J. E.; Hratchian, H. P.; Cross, J. B.; Bakken, V.; Adamo, C.; Jaramillo, J.; Gomperts, R.; Stratmann, R. E.; Yazyev, O.; Austin, A. J.; Cammi, R.; Pomelli, C.; Ochterski, J. W.; Ayala, P. Y.; Morokuma, K.; Voth, G. A.; Salvador, P.; Dannenberg, J. J.; Zakrzewski, V. G.; Dapprich, S.; Daniels, A. D.; Strain, M. C.; Farkas, O.; Malick, D. K.; Rabuck, A. D.; Raghavachari, K.; Foresman, J. B.; Ortiz, J. V.; Cui, Q.; Baboul, A. G.; Clifford, S.; Cioslowski, J.; Stefanov, B. B.; Liu, G.; Liashenko, A.; Piskorz, P.; Komaromi, I.; Martin, R. L.; Fox, D. J.; Keith, T.; Al-Laham, M. A.; Peng, C. Y.; Nanayakkara, A.; Challacombe, M.; Gill, P. M. W.; Johnson, B.; Chen, W.; Wong, M. W.; Gonzalez, C.; Pople, J. A. *Gaussian 03, Revision C.02*; Gaussian, Inc.: Wallingford, CT, 2004.
(64) Bayly, C. I.; Cieplak, P.; Cornell, W. D.; Kollman, P. A. *J. Phys. Chem.* **1993**, *97* (40), 10269–10280.
(65) Ponder, J. W. Tinker: Software Tools for Molecular Design, Version 4.2; 2004, http://dasher.wustl.edu/tinker/.
(66) Plimpton, S. *J. Comput. Phys.* **1995**, *117*, 1–19;http://lammps.sandia.gov.
(67) Martinez, L.; Andrade, R.; Birgin, E. G.; Martinez, J. M. *J. Comput. Chem.* **2009**, *30*, 2157–2164.
(68) Wang, J. M.; Wolf, R. M.; Caldwell, J. W.; Kollman, P. A.; Case, D. A. *J. Comput. Chem.* **2004**, *25* (9), 1157–1174.
(69) The parameters of amberff03_ua can be found in the package AmberTools 1.2. http://ambermd.org/.
(70) Koβmann, S.; Thar, J.; Kirchner, B.; Hunt, P. A.; Welton, T. *J. Chem. Phys.* **2006**, *124* (17), 174506.
(71) Bhargava, B. L.; Balasubramanian, S. *J. Chem. Phys.* **2005**, *123* (14), 144504.
(72) Micaelo, N. M.; Baptista, A. M.; Soares, C. M. *J. Phys. Chem. B* **2006**, *110* (29), 14444–14451.
(73) Tosi, M. P.; Fumi, G. *J. Phys. Chem. Solids* **1964**, *25*, 31–43.
(74) Fannin, A. A.; Floreani, D. A.; King, L. A.; Landers, J. S.; Piersma, B. J.; Stech, D. J.; Vaughn, R. L.; Wilkes, J. S.; Williams, J. L. *J. Phys. Chem.* **1984**, *88* (12), 2614–2621.
(75) Huddleston, J. G.; Visser, A. E.; Reichert, W. M.; Willauer, H. D.; Broker, G. A.; Rogers, R. D. *Green Chem.* **2001**, *3* (4), 156–164.
(76) Gomez, E.; Gonzalez, B.; Dominguez, A.; Tojo, E.; Tojo, J. *J. Chem. Eng. Data* **2006**, *51* (2), 696–701.
(77) Remsing, R. C.; Hernandez, G.; Swatloski, R. P.; Massefski, W. W.; Rogers, R. D.; Moyna, G. *J. Phys. Chem. B* **2008**, *112* (35), 11071–11078.
(78) Daivis, P. J.; Evans, D. J. *J. Chem. Phys.* **1994**, *100* (1), 541–547.
(79) Mondello, M.; Grest, G. S. *J. Chem. Phys.* **1997**, *106* (22), 9327–9336.
(80) Chen, T.; Smit, B.; Bell, A. T. *J. Chem. Phys.* **2009**, *131* (24), 246101.

JP911337F